Available online at www.sciencedirect.com
ScienceDirect
Ceramics International 36 (2010) 1117–1123
CERAMICS INTERNATIONAL
www.elsevier.com/locate/ceramint

Formation of nanosize ZnO particles by thermal decomposition of zinc acetylacetonate monohydrate

Svetozar Musić [a,*], Ankica Šarić [a], Stanko Popović [b]

[a] Division of Materials Chemistry, Ruđer Bošković Institute, P.O. Box 180, HR-10002 Zagreb, Croatia
[b] Department of Physics, Faculty of Science, University of Zagreb, P.O. Box 331, HR-10002 Zagreb, Croatia

Received 6 October 2009; received in revised form 2 November 2009; accepted 26 November 2009
Available online 4 January 2010

Abstract

Formation of ZnO particles by thermal decomposition of zinc acetylacetonate monohydrate in air atmosphere has been investigated using XRD, DTA, FT-IR, and FE-SEM as experimental techniques. ZnO as a single phase was produced by direct heating at ≥200 °C. DTA in air showed an endothermic peak at 195 °C assigned to the ZnO formation and exothermic peaks at 260, 315 and 365 °C, with a shoulder at 395 °C. Exothermic peaks can be assigned to combustion of an acetylacetonate ligand released at 195 °C. ZnO particles prepared at 200 °C have shown no presence of organic species, as found by FT-IR spectroscopy. Particles prepared for 0.5 h at 200 °C were in the nanosize range from ∼20 to ∼40 nm with a maximum at 30 nm approximately. The crystallite size of 30 nm was estimated in the direction of the a_1 and a_2 crystal axes, and in one direction of the *c*-axis it was 38 nm, as found with XRD. With prolonged heating of ZnO particles at 200 °C the particle/crystallite size changed little. However, with heating temperature increased up to 500 or 600 °C the ZnO particle size increased, as shown by FE-SEM observation. Nanosize ZnO particles were also prepared in two steps: (a) by heating of zinc acetylacetonate monohydrate up to 150 °C and distillation of water and organic phase, and (b) with further heating of so obtained precursor at 300 °C.

Keywords: A. Powders: Chemical preparation; B. Electron microscopy; B. X-ray methods; D. ZnO

1. Introduction

Zinc oxide (ZnO) has found many important applications. For example, ZnO powders are used in the production of varistors, paints, rubbers, cosmetics, or catalysts, whereas ZnO films are used in UV LEDs, acoustic wave devices, transparent electrodes, etc. The size and morphology of ZnO particles play an important role in these applications. Along with other physical and chemical properties, they can be changed or modified by using different routes of the synthesis of ZnO particles. ZnO can be generally synthesized using (a) crystallization in aqueous media at room temperature (RT) or under autoclaving conditions, (b) the microemulsion method, and (c) thermal decomposition of various Zn-containing compounds. Vacuum techniques are suitable for the preparation of ZnO films.

Thermal decomposition of zinc acetylacetonate, (Zn(acac)$_2$), was already utilized in the production of ZnO films. Notwithstanding the simplicity of this method, the mechanism of thermal decomposition of zinc acetylacetonate is complex [1]. The presence of H_2O molecules in Zn(acac)$_2$ crystals additionally complicates the mechanism of this reaction. Depending on the experimental parameters, this reaction yields ZnO particles of very different sizes and morphologies.

Fiddes et al. [2] prepared ZnO films by spray pyrolysis of an alcoholic solution of Zn(acac)$_2$·H_2O. Electrical resistivity of ZnO films depended on the temperature of pyrolysis, the presence of a water molecule in the starting chemical, and the atmosphere. Kashiwaba et al. [3] prepared ZnO films by chemical vapor deposition (CVD), using Zn(acac)$_2$ and oxygen as reactants. The cathodoluminescence spectra of ZnO films showed a strong peak of band edge luminescence at 379 nm and a very weak green emission in the visible region at ∼600 nm.

Transparent conducting ZnO thin films were prepared on glass substrates by CVD using zinc acetylacetonate as a starting chemical [4]. H_2O and H_2O_2 were found to be better oxygen

* Corresponding author. Tel.: +385 1 456 1094; fax: +385 1 46 80 098.
E-mail address: music@irb.hr (S. Musić).

0272-8842/$36.00
doi:10.1016/j.ceramint.2009.12.008

sources than air. Highly conductive undoped and Al-doped ZnO films were prepared by CVD at atmospheric pressure using zinc and aluminium acetylacetonates [5]. Ga-doped [6] and In-doped [7] ZnO films have also shown a high electrical conductivity. In these preparations [5,6] zinc acetylacetonate was used as the starting chemical.

Wu et al. [8] reported the formation of ZnO–Zn coaxial nanocables and ZnO nanotubes by thermal decomposition of zinc acetylacetonate on a silicon substrate. Kubota et al. [9] observed the formation of ZnO whiskers during evaporation of zinc acetylacetonate in oxygen atmosphere, followed by its thermal decomposition. The obtained whiskers had diameters of the cross-section ranging from 30 to 200 μm and lengths up to several hundreds of μm. Recently Yasuda and Segawa [10] conducted a similar investigation of the reaction between zinc acetylacetonate and oxygen at 450–700 °C.

Reference literature [1–10] showed a very strong dependence on the microstructure and physical properties of ZnO and ZnO-doped films produced from zinc acetylacetonate by modifying the thermal decomposition process. In the present work we have focused on the conditions for the formation of ZnO particles in powder form by thermal decomposition of zinc acetylacetonate monohydrate in air atmosphere. One of the objectives in the present work has been to investigate a possible formation of nanosize ZnO particles by this reaction. Generally, in technology of fine ZnO powders the thermal methods are more dominant than the ''wet'' chemical methods.

2. Experimental

Zinc acetylacetonate monohydrate ($Zn(C_5H_7O_2)_2{\cdot}H_2O$) was supplied by Alfa Aeser®. It was subjected to direct heating in air atmosphere, starting from RT to the proper temperature and heated for the period of time as given in Table 1 (samples S1 to S6). Then, the ceramic vessel with the solid thermal decomposition product was taken out from the furnace and left to cool at RT. Sample S7 was prepared in two steps: (a) by heating of acetylacetonate monohydrate up to 150 °C in distillation apparatus to remove H_2O and evaporable organic phase and (b) with further heating of so obtained precursor in ceramic vessel at 300 °C. Sample S8 was obtained with additional heating of sample S7 at 600 °C for 2 h and 800 °C for 2 h.

Table 1
Experimental conditions for the thermal treatment of $Zn(acac)_2{\cdot}H_2O$ and XRD analyses of decomposition products.

Sample	Heating temperature/°C	Heating time/h	XRD analysis	Remark
S1	200	0.5	ZnO	BDL
S2	200	2	ZnO	BDL
S3	200	24	ZnO	BDL
S4	500	2	ZnO	LBDL
S5	500	24	ZnO	LBDL
S6	600	2	ZnO	SDL

Key: BDL, broadened diffraction lines; LBDL, little broadened diffraction lines; SDL, sharp diffraction lines.

X-ray powder diffraction (XRD) patterns of the samples were taken at RT using an automatic Philips diffractometer (model MPD 1880, Cu Kα radiation, graphite monochromator, proportional counter).

DTA of $Zn(acac)_2{\cdot}H_2O$ was recorded using a Netzsch equipment. $Zn(acac)_2{\cdot}H_2O$ was mixed with Al_2O_3 in w/w ratio 1:1, then heated in air in the ceramic vessel at a rate of 10 °C min^{-1}. The temperature was controlled by a Pt–PtRh (10%) thermocouple.

Fourier transform infrared (FT-IR) spectra were recorded at RT using a Perkin-Elmer spectrometer (model 2000). The FT-IR spectrometer was coupled with a personal computer and operated with the IRDM (Infrared Data Manager) program. The specimens were pressed into pellets using a spectroscopically pure KBr.

Thermal field emission scanning electron microscope (FE-SEM, model JSM-7000F) manufactured by JEOL Ltd. was used for the inspection of the particle size and shape.

3. Results and discussion

3.1. X-ray powder diffraction and DTA

All samples obtained by direct heating of $Zn(acac)_2{\cdot}H_2O$ at ≥200 °C were identified (Table 1) as a single phase containing ZnO [11] (e.g., cards no. 89-1397, 89-0511, 36-1451). ZnO crystallized in the space group $P6_3mc$ (186, hexagonal system, wurtzite-type structure), with the unit-cell parameters (average among six data cards in [11]: $a = 3.249(2)$ Å and $c = 5.206(1)$ Å). Samples prepared in the present work have shown practically the same parameters as those cited above, with deviations within the standard experimental error. A significant broadening of diffraction lines was observed for samples S1, S2 and S3 prepared at 200 °C, which can be assigned to the presence of very fine ZnO particles. With heating temperature increased up to 500 °C the broadening of diffraction lines decreased, whereas for sample S6 prepared at 600 °C sharp diffraction lines were observed. This is illustrated in Fig. 1 with characteristic parts of XRD patterns of samples S1 and S6. The formation of ZnO at 200 °C (samples S1 to S3) is consistent with the DTA measurement. Fig. 2 shows a DTA curve of $Zn(acac)_2{\cdot}H_2O$ recorded in air. A strong endothermic peak is visible at 195 °C, which can be assigned to the ZnO formation. From 225 to 480 °C there are several exothermic peaks which can be assigned to combustion of a released acetylacetonate ligand. The exothermic peaks are located at 260, 315 and 365 °C, with a shoulder at 395 °C, and they are located in that temperature region, as observed for some other metal acetylacetonates. These changes in the location of exothermic peaks can be generally assigned to the nature of the metal, as well as to the catalytic effect of the corresponding oxide or Me^0 formed prior to combustion of the acetylacetonate ligand. Musić et al. [12] recorded a DTA curve of $Ru(acac)_3$ in air and observed the superposition of several exothermic peaks in the temperature range from 185 to 305 °C. The exothermic peak at 210 °C was related to RuO_2 crystallization, whereas the exothermic peaks between 245 and 280 °C were associated with combustion of an acetylacetonate ligand,

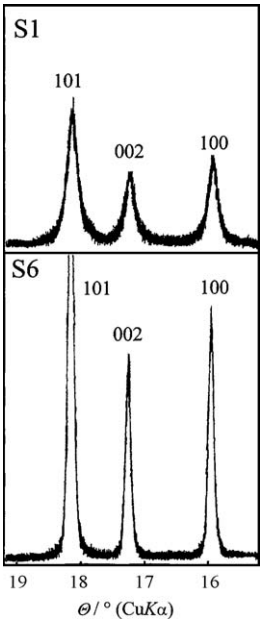

Fig. 1. Characteristic parts of XRD patterns of samples S1 and S6, recorded at RT.

probably in a few steps. Bykov et al. [13] used mass spectroscopy to investigate gaseous products released by thermal decomposition of $Ru(acac)_3$ in vacuum, hydrogen or oxygen; they found that in all three cases the initial thermal decomposition process was accompanied by the elimination of a free acetylacetonate ligand in the gas phase. Acetylacetonate was found as the major gaseous product between 300 and 350 °C, while above 400 °C the gaseous acetylacetonate ligand decomposed. The mass spectrum of the gaseous products released at 500 °C showed mainly CO, CO_2 and H_2O. DTA curve of $Ir(acac)_3$ in air showed several exothermic peaks between 245 and 325 °C, corresponding to decomposition of the acetylacetonate ligand in a gaseous phase [14]. Generally, the process of thermolysis of metal acetylacetonates plays an important role in the preparation of supported metal oxide catalysts. The initial concentration of the acetylacetonate complex, drying temperature and calcination are the factors which have a strong impact on the properties of oxide coatings, as shown in the cases of silica-supported vanadium oxide [15] and alumina-supported vanadium oxide [16] catalysts. The mechanism proposed for the formation of alumina-supported vanadium oxide catalyst [16] involves several steps. $VO(acac)_2$ complexes adsorbed onto an Al_2O_3 carrier were during a proton assisted thermolysis at 150 °C converted into covalently bonded species, i.e., an acetylacetonate ligand evolved into acetylacetone. The remaining acetylacetonate ligand was decomposed at 250–275 °C, with a release of acetone and CO_x. Al-acac species which were also present in the starting precursor converted at 275 °C into Al-acetate, which further decomposed at 325 °C.

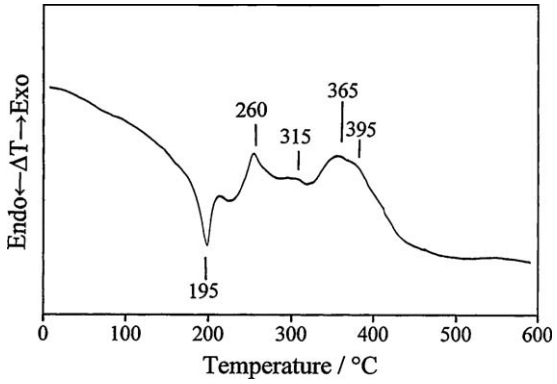

Fig. 2. DTA curve recorded for $Zn(acac)_2 \cdot H_2O$ in air atmosphere.

3.2. FT-IR spectroscopy

Samples S1 to S6 were also characterized by FT-IR spectroscopy and the corresponding spectra are shown in Fig. 3. The spectrum of sample S1 is characterized by a very broad IR band centered at 452 cm^{-1}. The shape of this IR band is similar to those in the spectra of samples S2 and S3. With heating temperature increased up to 500 °C (samples S4 and S5) two shoulders at 492 and 442 cm^{-1} were better pronounced, whereas the spectrum of sample S6 showed two resolved bands at 486 and 447 cm^{-1}, with a shoulder at 521 cm^{-1}. FT-IR spectroscopy has shown no organic bands in ZnO samples prepared at 200 °C, thus indicating that at these temperature ZnO particles are free from an acetylacetonate ligand. The IR spectrum of ZnO particles was the subject of previous investigations, because the shape of this spectrum is sensitive to particle size, particle aggregation and the type of ZnO polymorph. In many cases it is difficult to single out just one factor which influences the shape of the corresponding IR (or FT-IR) spectrum of ZnO particles. Hayashi et al. [17] recorded the IR transmission spectra of ZnO and compared them with the calculated spectra. The authors have found that ZnO showed three distinct absorption peaks located between the bulk TO-phonon frequency ($\omega_{T\|}$) and LO-phonon frequency ($\omega_{L\perp}$).

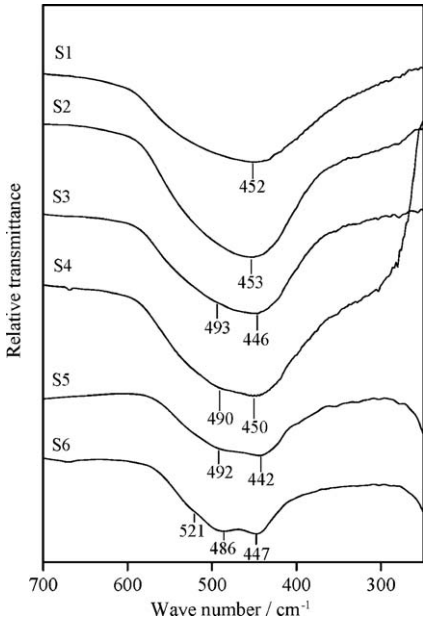

Fig. 3. FT-IR spectra of samples S1 to S6, recorded at RT.

These absorption peaks shifted towards lower frequencies when the permittivity of the surrounding medium was increased. Andrès-Vergès and Serna [18] showed that the IR spectrum of ZnO particles varied from a broad single band, over a doublet up to a three band superposition. Andrès-Vergès et al. [19] precipitated ZnO at elevated temperature from the solutions containing hexamethylenetetramine and $Zn(NO_3)_2$ or $ZnCl_2$. They have found that the geometrical shape of ZnO particles influenced the spectral shape in the corresponding IR spectrum. Tanigaki et al. [20] prepared cubic and hexagonal ZnO particles as well as tetrapod-shaped ZnO particles, and showed differences in their corresponding IR spectra.

3.3. FE-SEM

All samples were inspected with FE-SEM and selected FE-SEM images are shown in Figs. 4 and 5. Fig. 4 shows the FE-SEM images of ZnO samples: (a) S2, (b) S4, (c) S5 and (d) S6. The formation of very fine ZnO particles was noticed. The size of ZnO particles changed little with the heating time from 0.5 to 24 h at 200 °C. For example, in sample S1 the distribution of ZnO particle sizes covered a range from ∼20 to ∼40 nm with a maximum at ∼30 nm. The Scherrer method was used to estimate the crystallite size in sample S1. Selected diffraction lines were corrected for instrumental broadening. Pure broadening of diffraction lines 0 0 *l* was a little smaller than that of diffraction lines *h k* 0, indicating a small anisotropy in the crystallite shape. Estimated size in the direction of the a_1, a_2 crystal axes was 30(10) nm, whereas in one direction of the *c*-axis it was 38(12) nm. Taking into account the particle sizes in sample S1 as found by FE-SEM, it can be concluded that in the same sample the size of majority ZnO particles is very close to the crystallite sizes. The nanosize ZnO particles in sample S1 did not show the aggregation effect. With prolonged time of heating at 200 °C up to 2 h a slight increase of particle size from ∼25 to ∼50 nm (sample S2) was noticed. After 24 h of heating at the same temperature, the sizes of ZnO particles were ∼40 nm and higher (sample S3). FE-SEM image of sample S3 also showed the presence of aggregated ZnO particles. Fig. 4 also shows FE-SEM images of samples (b) S4, (c) S5 and (d) S6. ZnO particles produced at 500 °C for 2 h (sample S4) are visible (i) as distinct particles with size in the range of ∼40–100 nm and (ii) as aggregates of two or several of these particles. After 24 h of heating at 500 °C (sample S5), big aggregates in micron range are well visible. One such aggregate is shown in Fig. 4c. The effect of sintering is present. The same effect is observed in sample S6 (Fig. 4d) produced upon heating of zinc acetylacetonate monohydrate at 600 °C for 2 h.

Formation of ZnO at high temperatures yielded a variety of nanostructures, as reported in reference literature. In a review

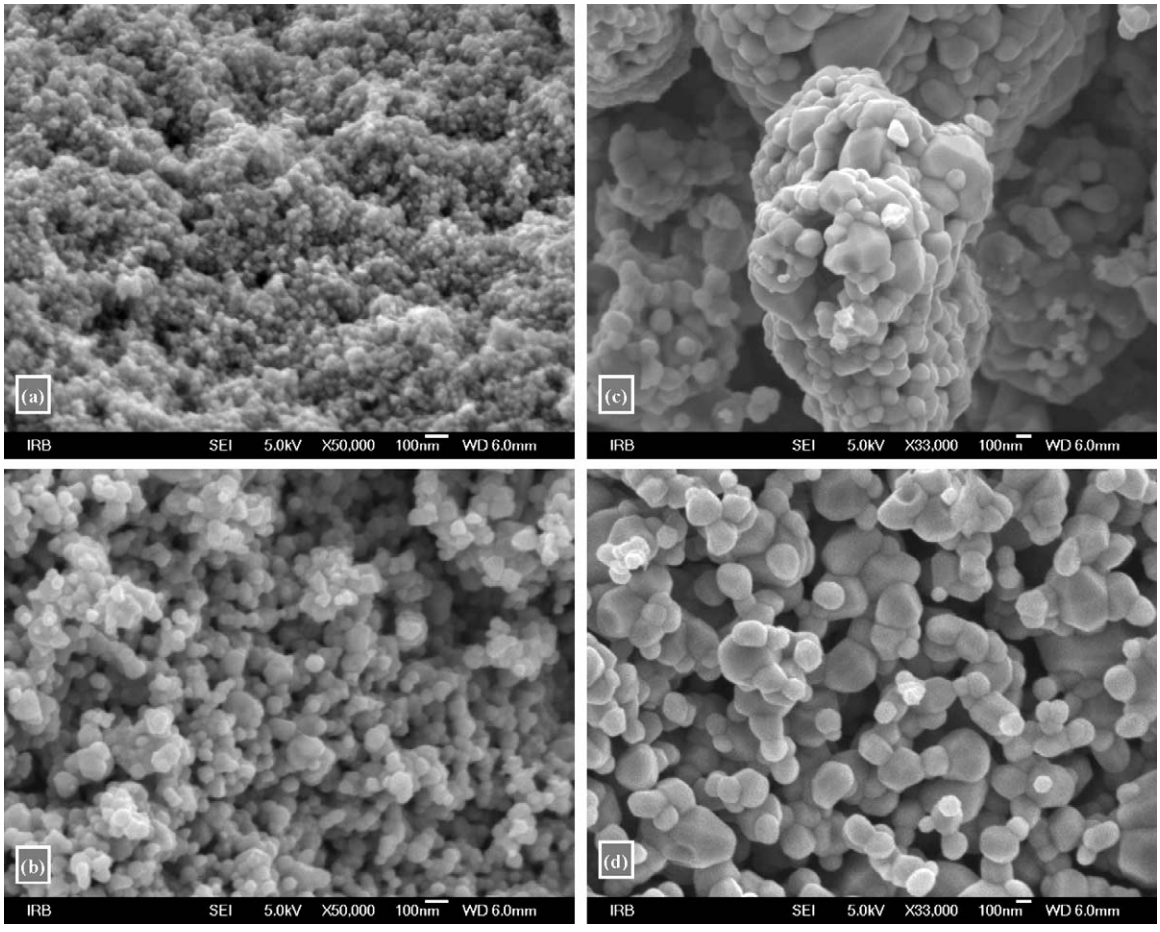

Fig. 4. FE-SEM images of samples: (a) S2, (b) S4, (c) S5 and (d) S6.

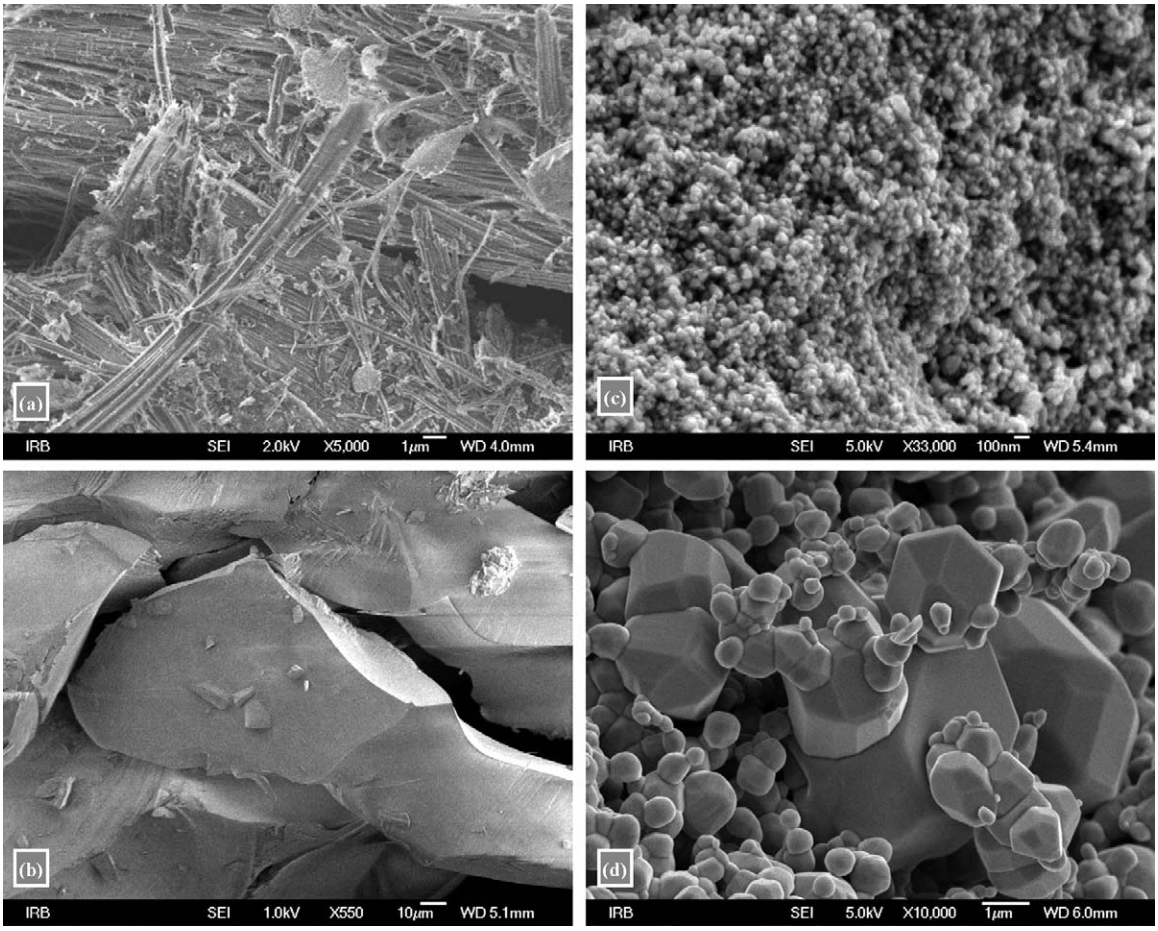

Fig. 5. FE-SEM images of samples: (a) starting zinc acetylacetonate monohydrate, (b) amorphous-like ZnO precursor obtained at 150 °C, (c) sample S7 and (d) sample S8.

by Wang [21] the formation of ZnO nanobelts, nanosprings, nanorings and nanopropellers by the solid–vapor deposition process was discussed. Formation of these nanostructures is a result of the three fastest growth directions, $\langle 0\,0\,0\,1\rangle$, $\langle 0\,1\,\bar{1}\,0\rangle$ and $\langle 2\,\bar{1}\,\bar{1}\,0\rangle$, and the polar surface induced phenomena. Formation of a specific nanostructure depends on the experimental parameters of the ZnO synthesis. Besides ZnO, the nanobelts of SnO_2, In_2O_3, Ga_2O_3, CdO and PbO were also produced by the solid–vapor deposition process [22]. Tetrapod-shaped ZnO whiskers were produced by the oxidation of metallic zinc at 500–800 °C under atmospheric pressure [23]. Sun et al. [24] prepared prismatic ZnO microtubes using the vapor transport method, i.e., by heating the mixture of ZnO and graphite powders in air, and the deposition on a silicon substrate covered by a copper grid, then the oxidation of Zn or ZnO_{1-x} by oxygen. Tseng et al. [25] used the same method to prepare ZnO nanowires by heating a 1:1 mixture of ZnO and Zn powders at 500 °C with trace water vapor as an oxidizer. Highly oriented ZnO nanostructures (ZnO–Zn coaxial nanocables, nanotubes, whiskers) could be obtained from zinc acetylacetonate precursor [8,9]. In the present work electron microscopy has shown no presence of these types of nanostructures. This difference can be attributed to the arrangement of our experiment, as well as the presence of hydrated water in zinc acetylacetonate used in the present work. Water enhanced thermal decomposition of zinc acetylacetonate by attacking with oxygen the carbonyl groups in acetylacetonate and/or starting a direct reaction with zinc.

Recently, the syntheses of nanosize ZnO particles by thermal decomposition of zinc acetylacetonate in oleylamine were published [26,27]. However, the advantages of oleylamine component, as well as the corresponding mechanism of ZnO formation were not elaborated.

The results of the present investigation showed sharpening of X-ray diffraction lines and gradual increase of particle size with increase of the heating temperature. The aggregation/sintering effect was specifically pronounced at 500 and 600 °C (samples S5 and S6). The FT-IR spectra of samples S1, S2 and S3 could be related to the FT-IR spectrum of nanosize ZnO particles synthesized by adding the tetramethylammonium hydroxide solution into the ethanolic solution of zinc acetate dihydrate [28]. On the other hand, the spectral shape of the FT-IR spectra of samples S5 and S6 can be considered as net effect of particle size and aggregation/sintering.

Fig. 5a shows FE-SEM image of zinc acetylacetonate monohydrate. The very long fibrils, laterally aggregated, are

well visible. Upon heating of zinc acetylacetonate monohydrate up to 150 °C and distillation of H_2O and vaporable organic phase, amorphous-like precursor of ZnO was obtained (Fig. 5b). Nanosize ZnO particles (∼40 nm in size) were obtained upon heating of amorphous-like precursor at 300 °C for 2 h (sample S7; Fig. 5c). Upon additional heating at 600 °C for 2 h and 800 °C for 2 h, sample S8 was produced and corresponding FE-SEM image is shown in Fig. 5d. This image shows a broad range of particle sizes in micron and submicron dimensions.

4. Conclusion

- Zinc acetylacetonate monohydrate, subjected to direct heating in air atmosphere between 200 and 600 °C, yielded ZnO as a single phase, as shown by XRD. The size of ZnO particles, produced for 0.5 h at 200 °C, covered a range from ∼20 to ∼40 nm with a maximum at about 30 nm. For the same sample, XRD indicated a small anisotropy in the crystallite shape, and by using the Scherrer method the crystallite size of 30 nm was estimated in the direction of the a_1 and a_2 crystal axes, whereas in one direction of the c-axis it was 38 nm. The particle/crystallite sizes changed little by heating up to 24 h at 200 °C.
- DTA in air showed an endothermic peak at 195 °C, which was assigned to the ZnO formation. The exothermic peaks at 260, 315 and 365 °C with a shoulder at 395 °C can be assigned to combustion of acetylacetonate ligand, which was released at 195 °C. FT-IR spectroscopy has not indicated the presence of organic species in ZnO particles prepared at 200 °C or at high temperatures.
- With heating temperature increased from 200 to 500 °C an increase in the size of ZnO particles was observed. Upon heating at 500 °C for 2 h the sizes of ZnO particles were in the range of ∼40–100 nm. After 24 h of heating at 500 °C ZnO particles in micron range were observed as a result of aggregation/sintering processes.
- Nanosize ZnO particles were also produced by combining (a) the heating of zinc acetylacetonate monohydrate up to 150 °C, distillation of H_2O and evaporable organic phase and (b) further heating of the precursor at 300 °C for 2 h. This route can be recommended as more suitable in production of nanosize particles.

References

[1] G.A.M. Hussien, Characterisation of the thermal genesis course of zinc oxide from zinc acetoacetonate dihydrate, Thermochimica Acta 186 (1991) 187–197.

[2] A.J.C. Fiddes, K. Durose, A.W. Brinkman, J. Woods, P.D. Coates, A.J. Banister, Preparation of ZnO films by spray pyrolysis, Journal of Crystal Growth 159 (1996) 210–213.

[3] Y. Kashiwaba, F. Katahira, K. Haga, T. Sekiguchi, H. Watanabe, Heteroepitaxial growth of ZnO thin films by atmospheric pressure CVD method, Journal of Crystal Growth 221 (2000) 431–434.

[4] H. Sato, T. Minami, T. Miyata, S. Takata, M. Ishii, Transparent conducting ZnO thin films prepared on low temperature substrates by chemical vapour deposition using $Zn(C_5H_7O_2)_2$, Thin Solid Films 246 (1994) 65–70.

[5] T. Minami, H. Sato, H. Sonohara, S. Takata, T. Miyata, I. Fukuda, Preparation of milky transparent conducting ZnO films with textured surface by atmospheric chemical vapour deposition using $Zn(C_5H_7O_2)_2$, Thin Solid Films 253 (1994) 14–19.

[6] Y. Kashiwaba, K. Sugawara, K. Haga, H. Watanabe, B.P. Zhang, Y. Segawa, Characteristics of c-axis oriented large grain ZnO films prepared by low-pressure MO-CVD method, Thin Solid Films 411 (2002) 87–90.

[7] A. Maldonado, M. de la Luz Olvera, r. Asomoza, S. Tirado-guerra, Highly conductive and transparent In-doped zinc oxide thin films deposited by chemical spray using $Zn(C_5H_7O_2)_2$, Journal of Materials Science: Materials in Electronics 12 (2001) 623–627.

[8] J.-J. Wu, S.-C. Liu, C.-T. Wu, K.-H. Chen, L.-C. Chen, Heterostructures of ZnO–Zn coaxial nanocables and ZnO nanotubes, Applied Physics Letters 81 (2002) 1312–1314.

[9] J. Kubota, K. Haga, Y. Kashiwaba, H. Watanabe, B.P. Zhang, Y. Segawa, Characteristics of ZnO whiskers prepared from organic-zinc, Applied Surface Science 216 (2003) 431–435.

[10] T. Yasuda, y. Segawa, Zinc oxide thin films synthesized by metal organic chemical reactions, Physica Status Solidi 241 (2004) 676–679.

[11] International Centre for Diffraction Data, Joint Committee on Powder Diffraction Standards, Powder Diffraction File, 1601 Park Lane, Swarthmore, PA, USA.

[12] S. Musić, S. Popović, M. Maljković, K. Furić, A. Gajović, Formation of RuO_2 and Ru by thermal decomposition of ruthenium(III)-acetylacetonate, Journal of Materials Science Letters 21 (2002) 1131–1134.

[13] A.F. Bykov, N.B. Morozova, I.K. Igumenov, S.V. Sysoev, Investigation of thermal properties of ruthenium(III) beta-diketonate precursors for preparation of RuO_2 films by CVD, Journal of Thermal Analysis 46 (1996) 1551–1565.

[14] S. Musić, S. Popović, M. Maljković, Ž. Skoko, K. Furić, A. Gajović, Thermochemical formation of IrO_2 and Ir, Materials Letters 57 (2003) 4509–4514.

[15] P. Van Der Voort, K. Possemiers, E.F. Vansant, Preparation of supported vanadium oxide catalysts: adsorption and thermolysis of vanadyl acetylacetonate on a silica support, Journal of the Chemical Society: Faraday Transactions 92 (1996) 843–848.

[16] M. Baltes, P. Van Der Voort, B.M. Weckhuysen, R.R. Rao, G. Catana, R.R. Schoonheydt, E.F. Vansant, Synthesis and characterization of alumina-supported vanadium oxide catalysts prepared by the molecular designed dispersion of $VO(acac)_2$ complexes, Physical Chemistry Chemical Physics 2 (2000) 2673–2680.

[17] S. Hayashi, N. Nakamori, H. Kanamori, Y. Yodogawa, K. Yamamoto, Infrared study of surface phonon modes in ZnO, CdS and BeO small crystals, Surface Science 86 (1979) 665–671.

[18] M. Andrès-Vergès, C.J. Serna, Morphological characterization of ZnO powders by X-ray and IR spectroscopy, Journal of Materials Science Letters 7 (1988) 970–972.

[19] M. Andrès-Vergès, A Mifsud, C.J. Serna, Formation of rod-like zinc oxide microcrystals in homogeneous solutions, Journal of the Chemical Society: Faraday Transactions 86 (1990) 959–963.

[20] T. Tanigaki, S. Kimura, N. Tamura, C. Kaito, A new preparation method of ZnO cubic phase particle and its IR spectrum, Japanese Journal of Applied Physics 41 (2002) 5529–5532.

[21] Z.L. Wang, Nanostructures of zinc oxide, Materials Today June (2004) 26–33.

[22] Z.R. Dai, Z.W. Pan, Z.I. Wang, Novel nanostructures of functional oxides synthesized by thermal evaporation, Advanced Functional Materials 13 (2003) 9–24.

[23] Z.W. Zhou, H. Deng, J. Yi, S.K. Liu, A new method for preparation of zinc oxide whiskers, Materials Research Bulletin 34 (1999) 1563–1567.

[24] X.W. Sun, S.F. Yu, C.X. Xu, C. Yuen, B.J. Chen, S. Li, Room-temperature ultraviolet lasing from zinc oxide microtubes, Japanese Journal of Applied Physics 42 (2003) L1229–L1231.

[25] Y.-K. Tseng, I.-N. Lin, K.-S. Liu, T.-S. Lin, I.-C. Chen, Low-temperature growth of ZnO nanowires, Journal of Materials Research 18 (2003) 714–718.

[26] J.F. Liu, Y.Y. Bei, H.P. Wu, D. Shen, J.Z. Gong, X.G. Li, Y.W. Wang, N.P. Jiang, J.Z. Jiang, Synthesis of relatively monodisperse ZnO nanocrystals from a precursor zinc 2,4-pentanedionate, Materials Letters 61 (2007) 2837–2840.

[27] M. Salavati-Niasari, F. Davar, M. Mazaheri, Preparation of ZnO nanoparticles from [bis(acetylacetonato)zinc(II)]-oleylamine complex by thermal decomposition, Materials Letters 62 (2008) 1890–1892.

[28] S. Musić, S. Popović, M. Maljković, Đ. Dragčević, Influence of synthesis procedure on the formation and properties of zinc oxide, Journal of Alloys and Compounds 347 (2002) 324–332.